ANL/EXT-08/32

Assessment of the Next Generation Nuclear Plant Intermediate Heat Exchanger Design

Nuclear Engineering Division

About Argonne National Laboratory

Argonne is a U.S. Department of Energy laboratory managed by UChicago Argonne, LLC under contract DE-AC02-06CH11357. The Laboratory's main facility is outside Chicago, at 9700 South Cass Avenue, Argonne, Illinois 60439. For information about Argonne, see www.anl.gov.

Availability of This Report

This report is available, at no cost, at http://www.osti.gov/bridge. It is also available on paper to the U.S. Department of Energy and its contractors, for a processing fee, from:

U.S. Department of Energy
Office of Scientific and Technical Information
P.O. Box 62
Oak Ridge, TN 37831-0062
phone (865) 576-8401
fax (865) 576-5728
reports@adonis.osti.gov

ANL/EXT-08-32

Assessment of the Next Generation Nuclear Plant Intermediate Heat Exchanger Design

by
S. Majumdar, A. Moisseytsev, and K. Natesan
Nuclear Engineering Division, Argonne National Laboratory

October 2008

Executive Summary

The Next Generation Nuclear Plant (NGNP), which is an advanced high temperature gas reactor (HTGR) concept with emphasis on production of both electricity and hydrogen, involves helium as the coolant and a closed-cycle gas turbine for power generation with a core outlet/gas turbine inlet temperature of 900-1000°C. In the indirect cycle system, an intermediate heat exchanger is used to transfer the heat from primary helium from the core to the secondary fluid, which can be helium, nitrogen/helium mixture, or a molten salt. The system concept for the vary high temperature reactor (VHTR) can be a reactor based on the prismatic block of the GT-MHR developed by a consortium led by General Atomics in the U.S. or based on the PBMR design developed by ESKOM of South Africa and British Nuclear Fuels of U.K.

This report has made an assessment on the issues pertaining to the intermediate heat exchanger (IHX) for the NGNP. A detailed thermal hydraulic analysis, using models developed at ANL, was performed to calculate heat transfer, temperature distribution, and pressure drop. Two IHX designs namely, shell and straight tube and compact heat exchangers were considered in an earlier assessment. Helical coil heat exchangers were analyzed in the current report and the results were compared with the performance features of designs from industry. In addition, a comparative analysis is presented between the shell and straight tube, helical, and printed circuit heat exchangers from the standpoint of heat exchanger volume, primary and secondary sides pressure drop, and number of tubes.

The IHX being a high temperature component, probably needs to be designed using ASME Code Section III, Subsection NH, assuming that the IHX will be classified as a class 1 component. With input from thermal hydraulic calculations performed at ANL, thermal conduction and stress analyses were performed for the helical heat exchanger design and the results were compared with earlier-developed results on shell and straight tube and printed circuit heat exchangers.

Contents

Acronyms

ANL	Argonne National Laboratory
ASME	American Society of Mechanical Engineers
DOE	Department of Energy
FEA	Finite Element Analysis
FEM	Finite Element Modeling
GA	General Atomics Company
GT-MHR	Gas Turbine - Modular Helium Reactor
HCHX	Helical Coil Heat Exchanger
HTGR	High Temperature Gas Reactor
HX	Heat Exchanger
ID	Inside Diameter
IHX	Intermediate Heat Exchanger
NGNP	Next Generation Nuclear Plant
OD	Outside Diameter
PBMR	Pebble Bed Modular Reactor
PCHE	Printed Circuit Heat Exchanger
PCS	Power Conversion System
UTS	Ultimate Tensile Strength
VHTR	Very High Temperature Reactor System

Figures

Tables

Assessment of the Next Generation Nuclear Plant Intermediate Heat Exchanger Design

1. Introduction

In the coming decades, the United States and the entire world will need energy supplies to meet the growing demands due to population increase and increase in consumption due to global industrialization. One of the reactor system concepts, the Very High Temperature Helium Cooled Reactor System (VHTR) has been identified as uniquely suited for producing hydrogen without consumption of fossil fuels or the emission of greenhouse gases [Generation IV 2002]. The U.S. Department of Energy (DOE) has selected this system for the Next Generation Nuclear Plant (NGNP) Project, to demonstrate emissions-free nuclear-assisted electricity and hydrogen production within the next 15 years.

The NGNP reference concepts are helium-cooled, graphite-moderated, thermal neutron spectrum reactors with a design goal outlet helium temperature of ≈1000°C [MacDonald et al. 2004]. The reactor core could be either a prismatic graphite block type core or a pebble bed core. The use of molten salt coolant, especially for the transfer of heat to hydrogen production, is also being considered. The NGNP is expected to produce both electricity and hydrogen. The process heat for hydrogen production will be transferred to the hydrogen plant through an intermediate heat exchanger (IHX).

The basic technology for the NGNP has been established in the former high temperature gas reactor (HTGR) and demonstration plants (DRAGON, Peach Bottom, AVR, Fort St. Vrain, and THTR). In addition, the technologies for the NGNP are being advanced in the Gas Turbine-Modular Helium Reactor (GT-MHR) project, and the South African state utility ESKOM-sponsored project to develop the Pebble Bed Modular Reactor (PBMR). Furthermore, the Japanese HTTR and Chinese HTR-10 test reactors are demonstrating the feasibility of some of the planned components and materials.

The proposed high operating temperatures in the VHTR place significant constraints on the design of the IHX as well as the thermal hydraulic and component material performance and ASME Code compliance. The focus of this assessment is to perform thermal hydraulic calculations for helium-to-helium heat exchanges for shell and straight tube, shell and helical tube, and printed circuit designs. The IHX being a high temperature component, probably needs to be designed using ASME Code Section III, Subsection NH, assuming that the IHX will be classified as a class 1 component. With input from thermal hydraulic calculations performed at ANL, thermal conduction and stress analyses were performed for HXs of different designs.

2. Intermediate Heat Exchanger Requirements

Several different potential plant design configurations for the NGNP with either direct or indirect power conversion cycles and integrated IHX designs were proposed and evaluated by Davis et al. [2005]. These configurations included IHX designs in parallel or in series with the NGNP power conversion system. In the serial designs, the total primary system flow from the reactor outlet passes through the IHX where approximately 50 MWt is transferred to the intermediate loop to drive the hydrogen production process. In these designs, heat is extracted from the primary fluid at the highest possible temperature (the reactor outlet temperature) for delivery to the hydrogen production process, while the power conversion system receives a

slightly lower temperature fluid. In the parallel designs, the flow from the reactor outlet is split, with a small fraction of the flow (approximately 10%) going to the IHX to drive the hydrogen production process, while the majority of the flow is delivered to the power conversion system for electrical power production. In these designs, both the hydrogen production process and the power conversion system receive the highest possible temperature fluid. Harvego [2006] has discussed the possible configurations for the design of IHX for NGNP and established the pros and cons of each configuration. Based on the design, he also established the flow rates, temperatures distribution through the loops, and other IHX requirements. Based on results from his study, we selected 900°C reactor outlet temperature as the base case in the earlier study [Natesan et al 2006].

The purpose of the IHX in NGNP is to transfer the heat from the nuclear reactor to the hydrogen production facility. Due to safety concerns, the hydrogen production facility cannot be integrated into the nuclear power production plant and the heat generated in the reactor may need to be transported over significant distances to the hydrogen production plant [Lillo et al. 2005]. The IHX must be robust enough to effectively transfer the heat from the reactor outlet helium at 900-1000°C to the secondary system. The hydrogen production facility requires a minimum temperature of 800°C for the thermochemical production of hydrogen (e.g., Sulfur-Iodine cycle) and about 700°C for high temperature electrolysis of water [Independent Technology Review Group 2004]. Therefore, the components of the heat transport system will be subjected to elevated temperatures for long times where adequate and reliable performance of materials is critical. This report presents a comparative analysis of heat transfer characteristics and component/material performance of different designs.

2.1 IHX Design Concepts

Three potential IHX design concepts, namely shell and straight tube, shell and helical tube, and printed circuit compact heat exchangers, are proposed for the transfer of heat from the primary helium to the secondary system. Compared to shell and tube heat exchangers, the compact HXs are characterized by a large heat transfer area per unit volume of the exchanger, resulting in reduced space, weight, support structure, and material cost.

The shell and tube exchanger is generally built of round tubes in a cylindrical shell with the tube axis parallel to that of the shell. One fluid flows inside the tubes and the other flows across and along the tubes. The major components of this exchanger are tubes, shell, front-end head, rear-end head, baffles, and tubesheets. Two of the three industrial teams, General Atomics [2008] and AREVA [2008], have proposed the use of helical coil heat exchanger (HCHX) as an intermediate heat exchanger (IHX) for primary-to-intermediate helium heat transfer for NGNP. The helical coil heat exchanger design however was not considered in the previous study [Natesan et al 2006]. Therefore, a computational model for the HCHX was developed for the present study.

Compact heat exchangers or printed circuit heat exchangers, which can substantially reduce the size of the unit for a given thermal capacity, have the potential for application in NGNP system. Additional details on such exchangers were discussed in an earlier report [Natesan et al 2006].

Model Description

A thermal hydraulic model was developed to calculate heat transfer, temperature distribution, and pressure drop inside a heat exchanger (HX). The model is one dimensional,

meaning that it is assumed that all channels on one side are identical and the calculations are done for one hot channel and one cold channel. Thus, any edge effects, such as heat losses though HX outside surface, are ignored. The model also assumes that the flow inside the HX is counter-flow, i.e. any heat transfer in flow distribution regions is ignored. Also the model is for single-phase fluids only and it is assumed that there is no phase transition inside the HX.

The model takes into account the fluid properties variation along the channel length. The channel length is divided into a number of regions. Inside each region the fluid properties are assumed to be constant, but the properties vary from region to region. For each region the heat transfer equations are solved to calculate the temperature changes in the region for both fluids. Also, the pressure drop for each region is calculated. The heat transfer equations, as well as their solution are described elsewhere [Moisseytsev 2003].

The input data for the model include:

- Hot and cold side fluids,
- Hot and cold side inlet conditions (temperature and pressure),
- Hot and cold side flow rates,
- Number of HX units and unit dimensions (length, height and width, or diameter),
- HX-type specific information to describe the channel geometry (e.g., tube inner and outer diameter, tube pitch, etc.),
- HX (tube) material,
- Heat transfer correlation to use,
- Number of regions along the channel, and
- Required accuracy of the calculation.

The output data (results) of the model are:

- Hot and cold sides outlet temperatures and pressures,
- HX heat duty, and
- Pressure and temperature distribution along the channel inside the heat exchanger.

2.1.1 Helical Coil Heat Exchanger

The HCHX model, developed for this study, is based on the earlier developed shell-and-tube heat exchanger model [Natesan et al 2006]. The model is designed to calculate the heat transfer and pressure drop on both sides of the heat exchanger. It is a one-dimensional multi-node single-phase design model that takes into account the variation in properties of the two fluids and thermal conductivity of tube wall with temperature and pressure. Even though there are several ways in which the model can be used for the heat exchanger design calculations, in the present study the inlet conditions (temperature, pressure, and flow rate) are specified for both fluids as well as the desired hot side outlet temperature. The model then iterates on the heat exchanger dimensions (tube bundle height for HCHX) to match the required outlet conditions. The main outputs from the model include the required heat exchanger dimensions as well as outlet temperatures and pressure drops for both sides. Also, as a result of the calculations, the detailed distributions of pressure, temperature and other parameters (such as heat transfer coefficients, for example) inside the heat exchanger are available.

The previous shell-and-tube heat exchanger model was modified to enable HCHX calculations. The modifications include the helical coil geometry treatment as well as

introduction of heat transfer and pressure drop correlations for helical coil. These modifications are briefly discussed below.

The implementation of the HCHX model follows the recommendations described in Reference [Smith 1997]. The simplified HCHX geometry is shown in Fig. 2.1. The HCHX in Fig. 2.1 has three coils (group of tubes at the same diameter *D*). The example in Figure 2.1 also demonstrates that the number of tubes per coil varies from coil to coil (three tubes for outer coil, four for middle coil and five for inner coil in Fig. 2.1). Figure 2.1 also defines the axial (*t*) and vertical (*p*) pitches as tube center-to-tube center distances between coils and tubes in the same coil, respectively. It is assumed in Fig. 2.1 and in the model that all tubes have the same diameter and wall thickness. It is also assumed in the model (consistent to designs in References [General Atomics 2008, Areva 2008] that the helix angle of coil, φ, (measured to the horizontal axis) is constant for all tubes.

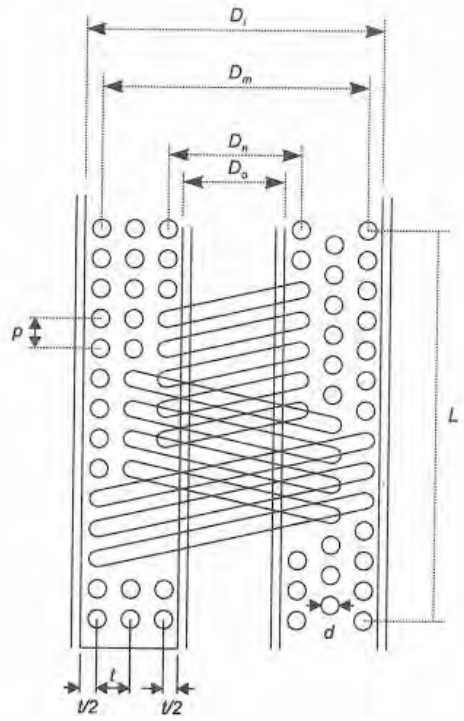

Figure 2.1. Helical coil heat exchanger geometry [Smith 1997].

Similar to the previous models, the HCHX model calculates heat transfer and pressure drop in helical coil region only, i.e. any heat transfer and pressure drop in flow distributor regions are ignored. Figure 2.2 shows how the geometric parameters for HCHX model are calculated. The dotted line on the side view represents one tube among the several tubes for a coil. The bottom view shows only one tube per coil (for simplicity); in reality there would be several tubes per coil starting at different angular locations.

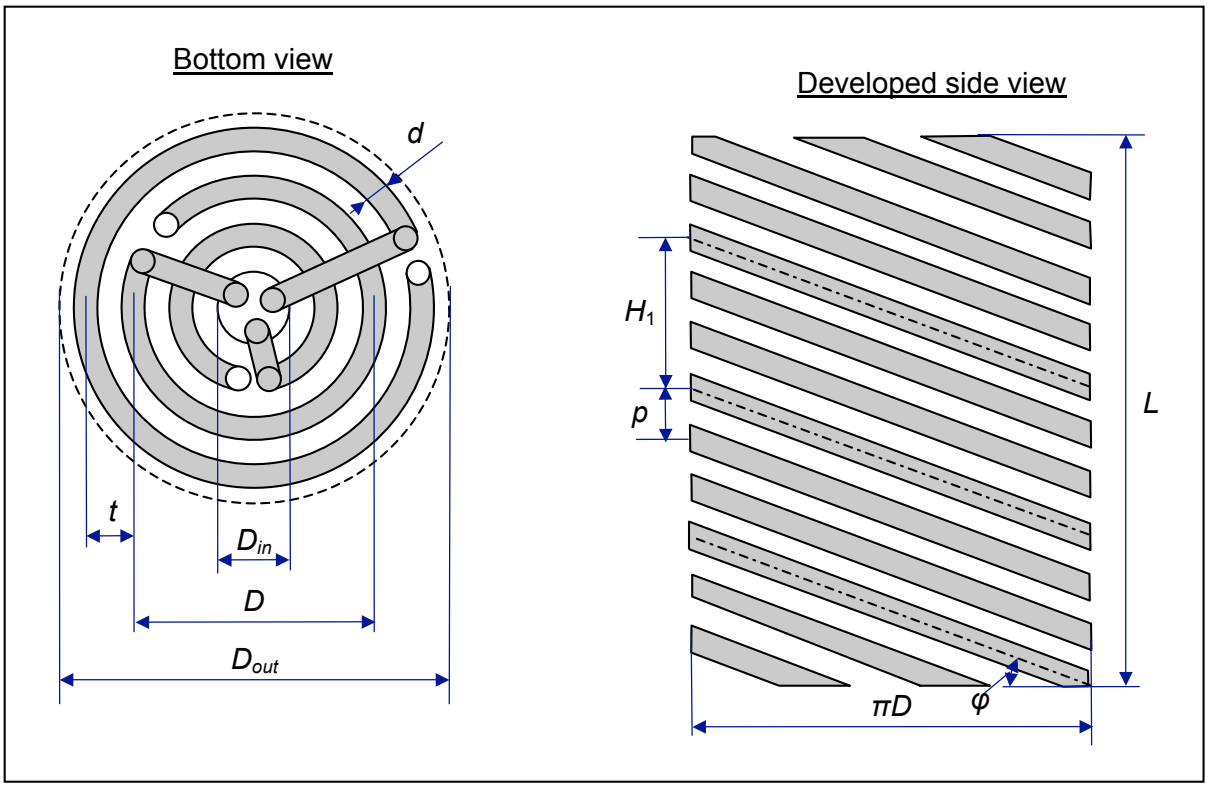

Figure 2.2. Helical coil heat exchanger geometry for the model.

The tube length in helical coil region is calculated as

$$l = \frac{L}{\sin\varphi} \ ,$$

where L = helical region height (Figs. 2.1 and 2.2).

Note that the tube length is the same for all coils since the helix angle is constant. The number of tube, N_t, for a coil of diameter D is calculated from the following relationships (Figure 2.2):

$$\tan\varphi = \frac{H_1}{\pi D}$$

$$H_1 = p \cdot N_t$$

thus

$$N_t = \frac{H_1}{p} = \frac{\pi D \tan\varphi}{p}$$

Of course, the number of tubes is an integer number, so the result of the equations above is rounded to the nearest integer to get a number of tubes for a coil. The coil diameter for coil is calculated as

$$D_i = D_1 + 2 \cdot t \cdot (i-1), \ i = 1 \ldots N_{coil}$$

where D_1 is the diameter of the innermost coil and the number of coils is defined as a maximum number i such that $D_i<D_{out}$.

The code calculates the heat transfer based on an "average" coil. The average coil is defined as a coil of average diameter $\overline{D}$ that is calculated as

$$\overline{D} = \frac{\sum_{i=1}^{N_{coil}} N_i D_i}{\sum_{i=1}^{N_{coil}} N_i}$$

The model assumes that the flow per tube is a total flow divided by the total number of tubes, i.e., it is assumed that the flow is distributed equally among all tubes.

The heat transfer calculations are performed for all tubes (rather than for one tube). That means that the flow rates are total flows for a heat exchanger, the heat transfer area is defined as a total surface area of all tubes, and the flow areas are defined as a total inside cross sectional area of all tubes for the tube side and the total available flow area (total area minus area blocked by tube coils) on the shell side. The total heat transfer (coil region) length is divided into a number of regions; the fluid and tube wall properties are assumed to be constant inside each region but are changing from region to region. The pressure drop on tube side is calculated based on flow per one tube.

The following heat transfer and pressure drop correlations [Smith 1997] are used in the model (Tables 2.1. and 2.2). In the model, the correlations are applied based on the average coil diameter calculated in the equation above.

Table 2.1. Heat transfer correlations for HCHX [Smith 1997]

	Laminar flow $(\mathrm{Re} < \mathrm{Re}_{tr})$	**Turbulent flow** $(\mathrm{Re} \geq \mathrm{Re}_{tr})$
Tube Side	$Nu = 0.864 \frac{\sqrt{De}}{\xi}\left[1 + \frac{2.35}{\sqrt{De}}\right]$ $\xi = \begin{cases} \frac{1}{5}\left[2 + \sqrt{10/\mathrm{Pr}^2 - 1}\right] & \mathrm{Pr} < 1 \\ \frac{2}{11}\left[1 + \sqrt{1 + 77/4\,\mathrm{Pr}^2}\right] & \mathrm{Pr} \geq 1 \end{cases}$	$Nu = \frac{\mathrm{Pr}\cdot \mathrm{Re}^{0.8}\left(\frac{d}{D}\right)^{0.1}\left[1 + \frac{0.098}{\mathrm{Re}\left(\frac{d}{D}\right)^2}\right]}{26.2\cdot \mathrm{Pr}^{0.666} - 0.074}$ for $\mathrm{Pr} < 1$ $Nu = \frac{\mathrm{Pr}^{0.4}\cdot \mathrm{Re}^{5/6}\left(\frac{d}{D}\right)^{1/12}\left[1 + \frac{0.061}{\left\{\mathrm{Re}\left(\frac{d}{D}\right)^{2.5}\right\}^{0.167}}\right]}{41}$ for $\mathrm{Pr} \geq 1$

Shell Side	$Nu = 0.332 \cdot \mathrm{Re}^{0.6} \cdot \mathrm{Pr}^{0.36}\ for\left(1\times10^{3} < \mathrm{Re} < 2\times10^{4}\right)$ $Nu = 0.123 \cdot \mathrm{Re}^{0.7} \cdot \mathrm{Pr}^{0.36}\ for\left(2\times10^{4} \le \mathrm{Re} < 2\times10^{5}\right)$ $Nu = 0.036 \cdot \mathrm{Re}^{0.8} \cdot \mathrm{Pr}^{0.36}\ for\left(2\times10^{5} \le \mathrm{Re} < 9\times10^{5}\right)$

Table 2.2. Friction factor correlations for HCHX [Smith 1997]

	Laminar flow $\left(\mathrm{Re} < \mathrm{Re}_{tr}\right)$	**Turbulent flow** $\left(\mathrm{Re} \ge \mathrm{Re}_{tr}\right)$
Tube Side	$\frac{f}{f_s} = \frac{21.5 \cdot De}{\left[1.56 + \log(De)\right]^{5.73}}$ $f_s = \frac{16}{\mathrm{Re}}$	$f = \frac{0.305\left\{1 + \frac{0.112}{\left[\mathrm{Re}\left(d/D\right)^2\right]^{0.2}}\right\}\sqrt{d/D}}{4\left[\mathrm{Re}\left(d/D\right)^2\right]^{0.2}}$
Shell Side	$f = P_y \cdot 0.26 \cdot \mathrm{Re}^{-0.117}$	

where

$\mathrm{Re}_{tr} = 2{,}300\left[1 + 8.6\left(d/D\right)^{0.45}\right]$ = laminar-turbulent transition Reynolds number,

$De = \mathrm{Re}\sqrt{d/D}$ = Dean number,

d = tube inner diameter,

D = coil diameter,

P_y = shell side porosity (fraction of shell inside volume not occupied by tubes).

Since the shell diameter for HCHX is defined by a number of coils, it could not be varied continuously (unlike the shell diameter in shell-and-tube heat exchanger). Therefore, the HCHX model is modified such that it calculates the required heat exchanger height (length) for the specified heat duty (versus shell diameter variation for shell-and-tube heat exchanger).

2.1.2 Comparison of the HCHX Model with GA and AREVA Results

The HCHX model has been applied to the helical coil HX designs reported by GA and AREVA.

Table 2.3 shows the comparison of the model results of for the GA PCS-side IHX with 18 coil layers (Tables 4-3 and 4-4 of Reference [General Atomics 2008]). Highlighted in yellow are the calculated results while the input parameters are shown in white. Overall, a close agreement is achieved by the HCHX model. The only significant differences are in pressure drops (the HCHX model calculates pressure drop in the helical coil (tube bundle) region only; it is not clear whether the GA results included the headers and distribution regions).

Table 2.4 shows the comparison of the model results for the AREVA tubular IHX for two-loop design (Table 5-7 of Reference [Areva 2008]). Similar to Table 2.3, highlighted in yellow are the calculated results while the input parameters are shown in white. Again, a close agreement is achieved by the HCHX model. For this design, however, some detailed design information is not reported in Reference [Areva 2008] and had to be estimated, based on some assumptions (such as the same horizontal and vertical pitches).

Since more detailed information is available for GA PCS-side IHX design, this design is selected for further analysis. Also, the comparison between different IHX designs, reported in consequent sections, is based on the conditions defined by this design.

Table 2.3. Comparison of the model results with GA design

Item		Unit	GA Design	Model
Number of units			3	3
Unit heat duty		MWt	178	178.4
Primary side	Fluid		He	He
	Side		Shell	Shell
	Inlet temperature	°C	900	900
	Flow rate	kg/s	81.80	81.80
	Outlet temperature	°C	480	480
	Inlet pressure	MPa	7.0	7.0
	Pressure drop	kPa	4	2.024
Secondary side	Fluid		He	He
	Side		Tube	Tube
	Flow rate	kg/s	87.64	87.64
	Inlet temperature	°C	308	308
	Outlet temperature	°C	700	700
	Inlet pressure	MPa	7.1	7.1
	Pressure drop	kPa	79	37.05
Tube	Outer diameter	mm	45	45
	Thickness	mm	5	5
	Tube length	m	22.05	22.14
	Number of tubes		550	552
Helically coiled tube bundle	Angle	deg	12	12
	Number of coils		18	18
	Diameter of inner coil	mm	1870	1870
	Diameter of outer coil	mm	4080	4080
	Horizontal pitch	mm	65	65
	Vertical pitch	mm	65	65
	Effective height	m	4.58	4.60
Velocity of primary He	High temperature region	m/s	11	8.29
	Middle temperature region	m/s	9.11	6.71
	Low temperature region	m/s	7.2	5.37
Velocity of secondary He	High temperature region	m/s	46.08	47.02
	Middle temperature region	m/s	36.66	36.80
	Low temperature region	m/s	27.36	28.23

Table 2.4. Comparison of the model results with AREVA design

Item		Unit	AREVA Design	Model
Unit heat duty		MWt	290	289.6
Primary side	Fluid		He	He
	Side		Shell	Shell
	Flow rate	kg/s	136	136
	Inlet temperature	°C	900	900
	Outlet temperature	°C	490	490
	Inlet pressure	MPa	5.0	5.0
	Pressure drop	MPa	0.02	0.023
Secondary side	Fluid		He	He
	Side		Tube	Tube
	Flow rate	kg/s	136	136
	Inlet temperature	°C	415	415
	Outlet temperature	°C	825	825
	Inlet pressure	MPa	5.5	5.5
	Pressure drop	MPa	0.2	0.183
Tube	Outer diameter	mm	21	21
	Thickness	mm	2.2	2.2
	Tube length	m	18.3	20.0 (18.2 for 7.8m H)
	Number of tubes		2,966	3,045
Helically coiled tube bundle	Angle	deg	25.38	25.38
	Number of coils			29
	Diameter of inner coil	mm	1,500	1,500
	Diameter of outer coil	mm	3,478	3,478
	Horizontal pitch	mm	35.3*	35.3*
	Vertical pitch	mm	35.3*	35.3*
	Effective height	m	7.8	8.55

* Data is not reported; estimated based on number of tubes, number of coils, and coil inner and outer diameters.

2.1.3 HCHX Model Results

From the thermal hydraulic calculations based on the HCHX design model, a detailed distribution of different parameters along the HX height is available. This information is used for stress analysis of helical coil heat exchanger. Figure 2.3 shows the example of this distribution for the fluid and tube wall temperatures, along with other calculated parameters, such as heat flux and thermal resistance.

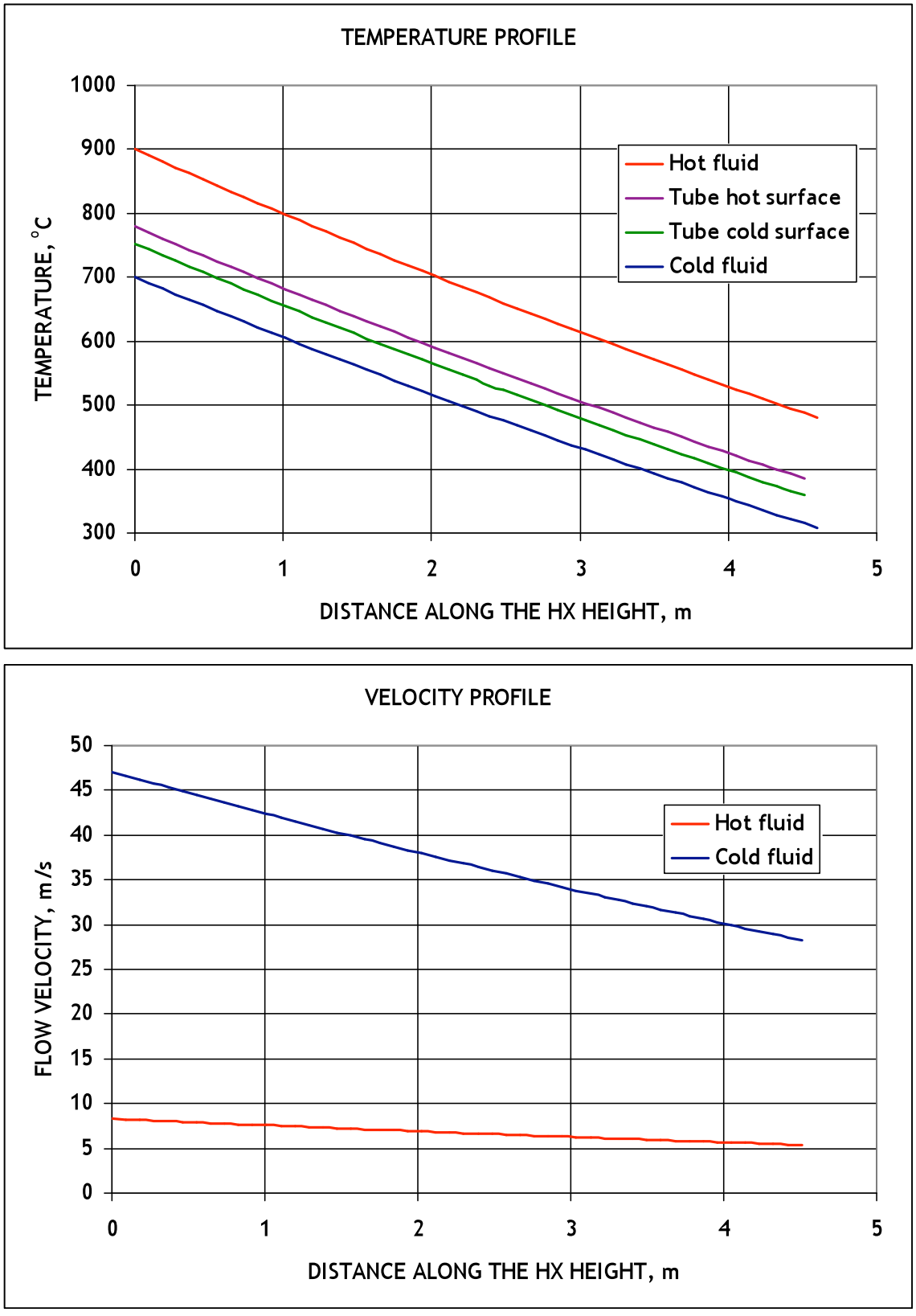

Figure 2.3. Calculated axial profiles for HCHX.

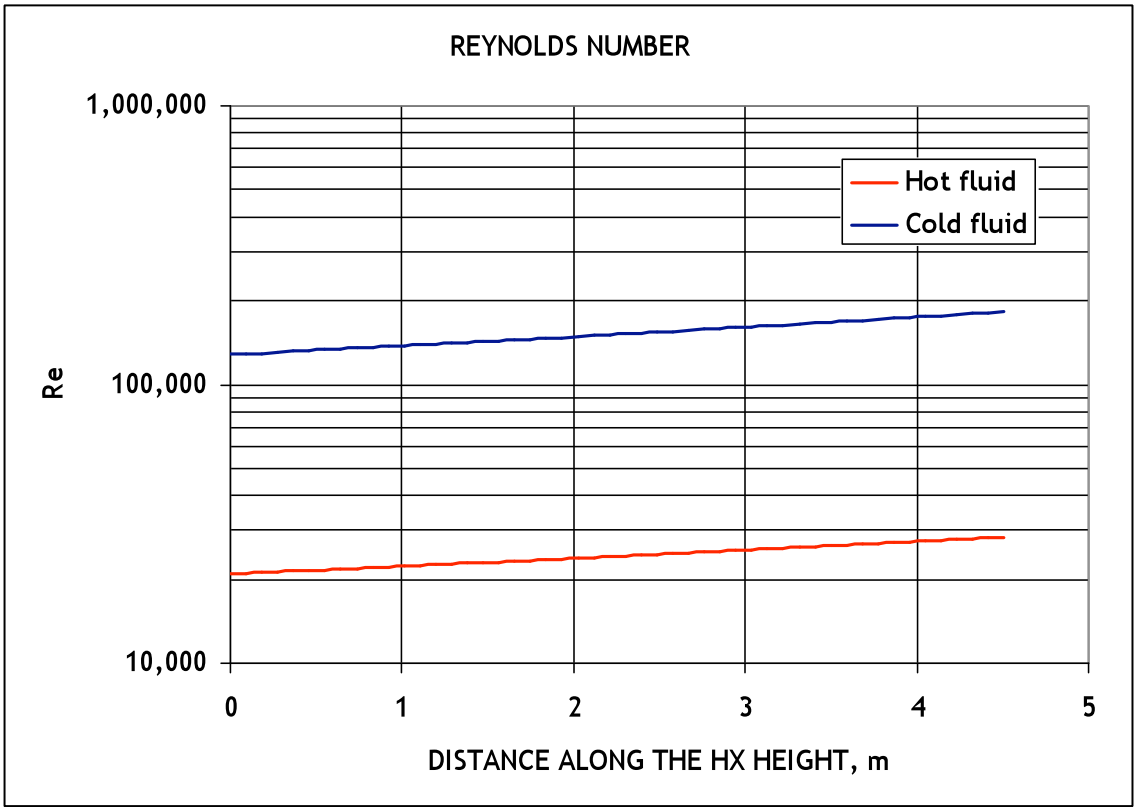

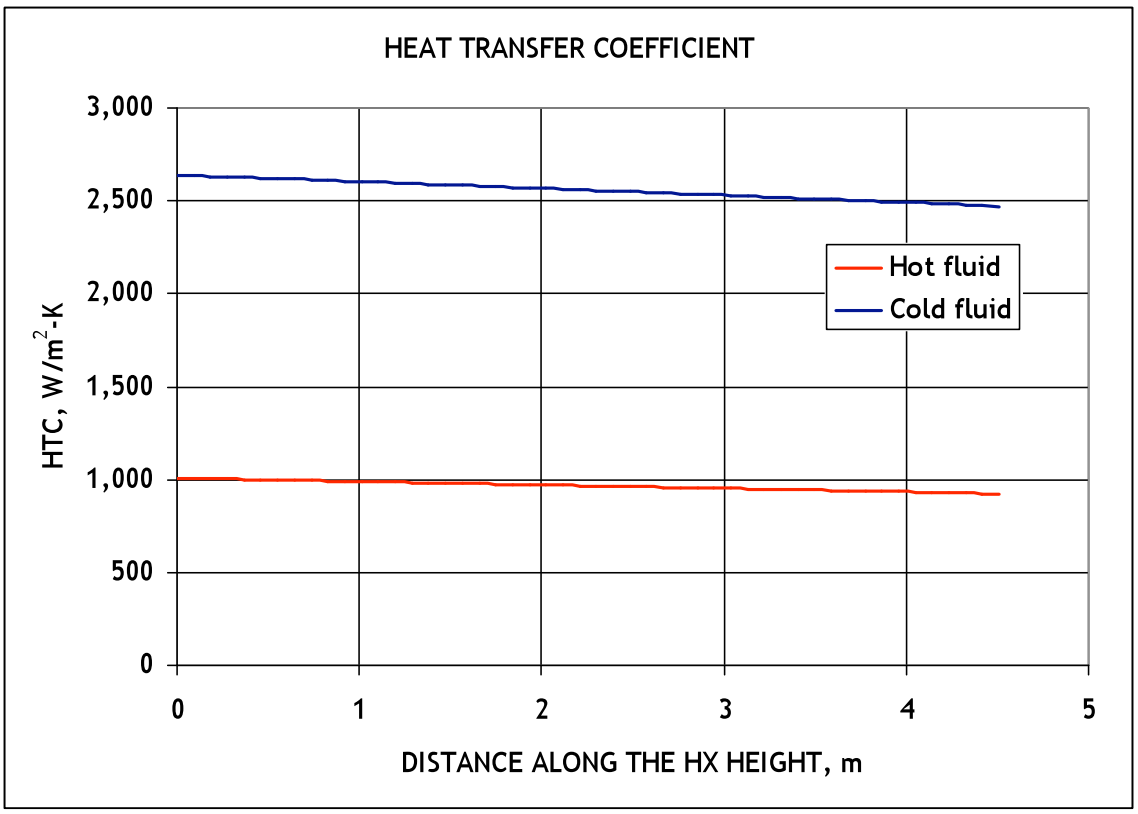

Figure 2.3. Calculated axial profiles for HCHX (Continued).

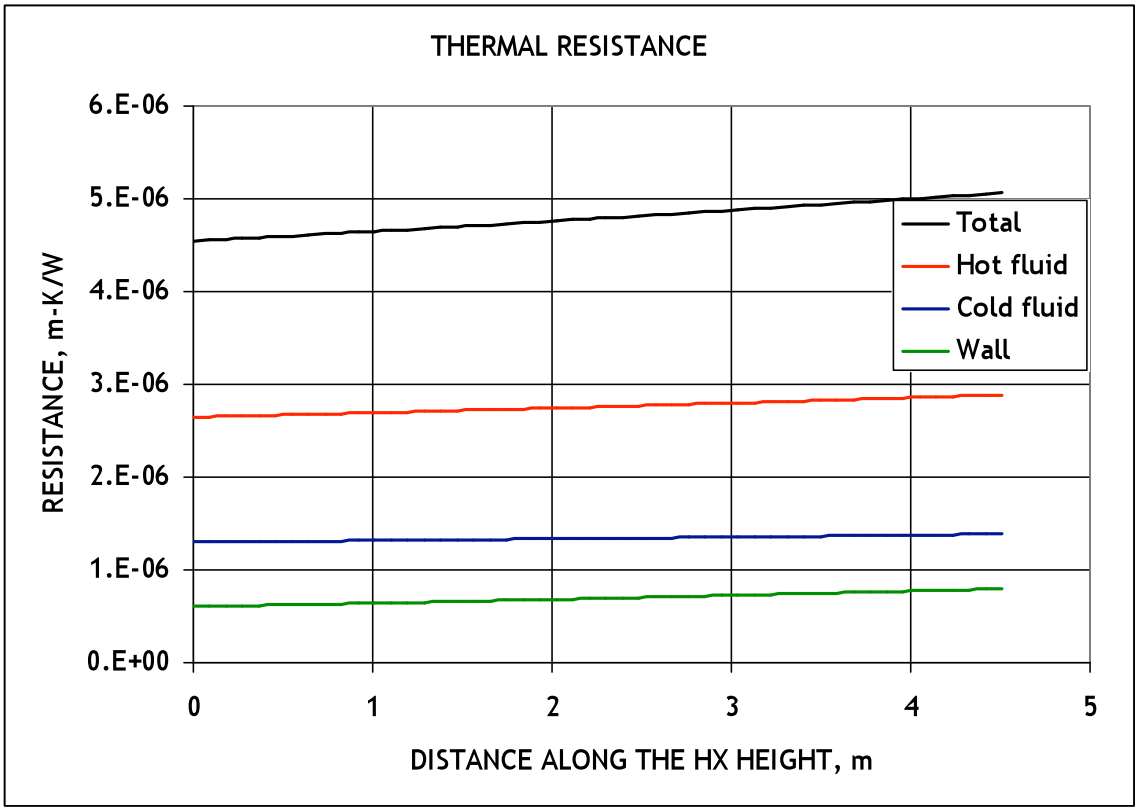

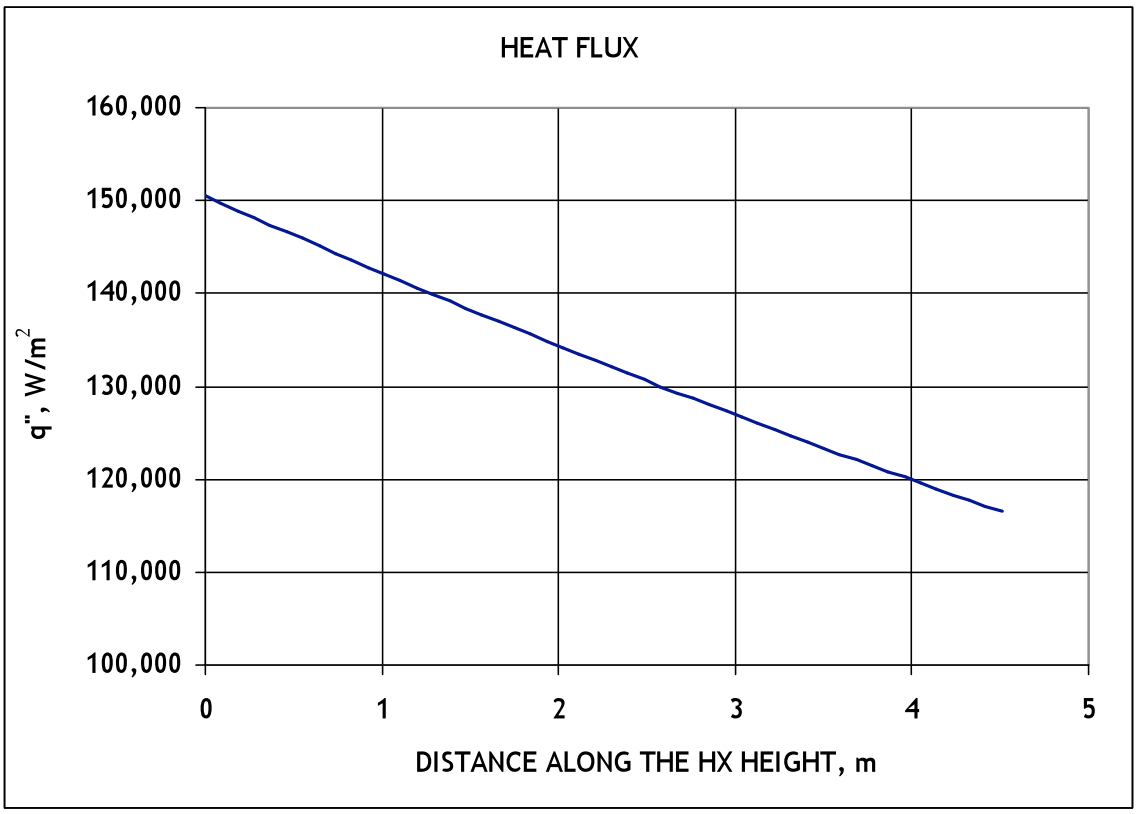

Figure 2.3. Calculated axial profiles for HCHX (Continued).

To estimate the effect of the temperature variation between different coils, the following analysis has been carried out. In addition to the average coil calculations, described above, the analysis has been repeated for coils representing the first (inner) and the last (outer) coils of the HCHX. The heat exchanger height is fixed in these calculations. Also fixed are the flow rates on shell and tube sides, i.e. any differences in flow variation between coils are ignored. This assumption was necessary due to one-dimensional nature of the code. It is expected that this assumption is the most limiting on the shell side, where the flow area between the coils increases with coil diameter such that the flow distribution between the coils would be expected. Table 2.5 shows the variation of the coil diameter and number of tubes by coil for the PCS-side design defined in Table 2.3.

Table 2.5. Variation of the parameters by coils

Coil Number	Coil Diameter (m)	Number of Tubes
1	1.87	19
2	2.00	21
3	2.13	22
4	2.26	23
5	2.39	25
6	2.52	26
7	2.65	27
8	2.78	29
9	2.91	30
10	3.04	31
11	3.17	33
12	3.30	34
13	3.43	35
14	3.56	37
15	3.69	38
16	3.82	39
17	3.95	41
18	4.08	42

Table 2.6 shows the comparison between the outlet temperatures for the first, average and the outer coils for the HCHX design and conditions defined in Table 2.3. The average coil conditions are those used in the design calculations so they are exactly the same as in Table 2.3. The variation in the heat flux and, therefore, the outlet temperatures is mostly due to dependency of the heat transfer correlations on the coil diameter (Table 2.1). The variation is pressure drop between the coils is minimal due to the fact the both HX height and tube length are the same for all coils, such that the difference in pressure drop are caused by properties (e.g., density) variation and friction factor dependency on the coil diameter only.

Table 2.6. Outlet temperatures (in °C) in different coils

	First coil	Average Coil	Last Coil
Primary side	478.2	480.0	480.9
Secondary side	701.8	700.0	699.1

It is noted again that the results in Table 2.6 were obtained from one-dimensional code under the fixed flow rate assumption. In detailed three-dimensional calculation, it is expected that the temperature variation would be more significant due to flow redistribution.

2.1.4 Shell-and-Straight Tube Heat Exchanger

To compare the shell-and-tube heat exchanger with helical coil HX, the design calculations, similar to those reported in previous work [Natesan et al 2006] have been carryout out for the PCS-side HX conditions defined in Table 2.3. The calculations are carried out for two different tube dimensions (diameter and thickness): those selected in previous work (1.0 cm ID, 2 mm wall) and those selected for HCHX design presented in Table 2.3 (3.5 mm ID, 5 mm wall). The pitch of the 1 cm tubes has been modified from previous results to match the pitch-to-diameter ratio of the HCHX design (p/d=1.444).

Figure 2.4 shows how the calculated design parameters vary with the selected tube length for 1 cm tube design. In general, longer tubes allow the smaller shell diameter and smaller total HX volume, but at expense of the pressure drop and possibly higher fabrication costs. Since the PCS-side IHX design requirements define maximum allowable pressure drop as 50 kPa for both sides (Table 4-3 of Reference [General Atomics 2008]), 4 m tubes are selected for this design. The resulting design and flow parameters are presented in Table 2.7 that compares all the considered concepts in Section 2.1.6 below.

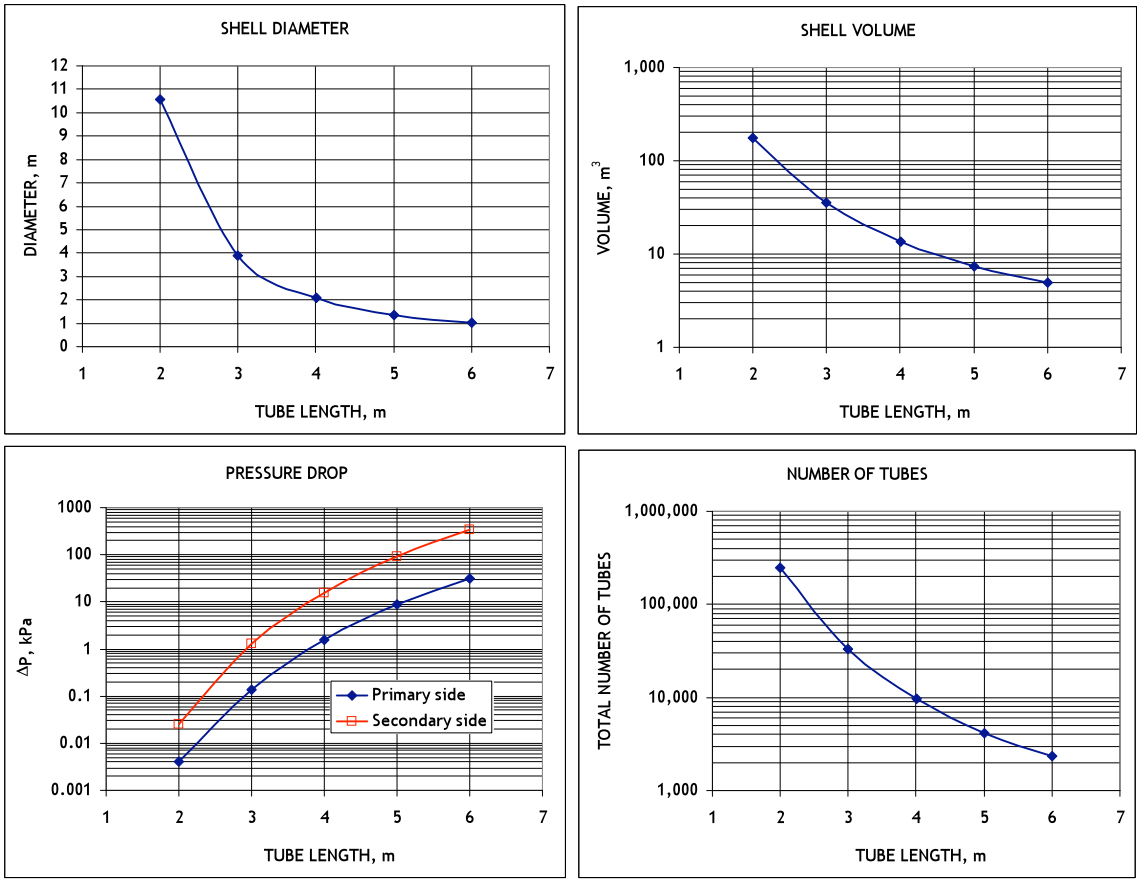

Figure 2.4. Shell-and-tube design sensitivity on the tube length for 1 cm tube.

Figure 2.5 shows the similar results for larger 3.5 cm tubes. It is expected that the larger tubes would require longer heat exchanger to achieve the equivalent heat transfer rate. In fact, the calculations show that for the tubes shorter than 10 m, the laminar flow regime is calculated such that very large heat exchanger would be required. Also the calculations have shown the results approach the HCHX parameters if tube length approaches that of the HCHX (≈20 m). Since the fabrication of 20+m-long heat exchanger would be problematic, 12 m tubes are selected for the comparison. Due to large tube diameter, the pressure drop stays small even for very long tubes such that pressure drop requirements do not limit the design choices.

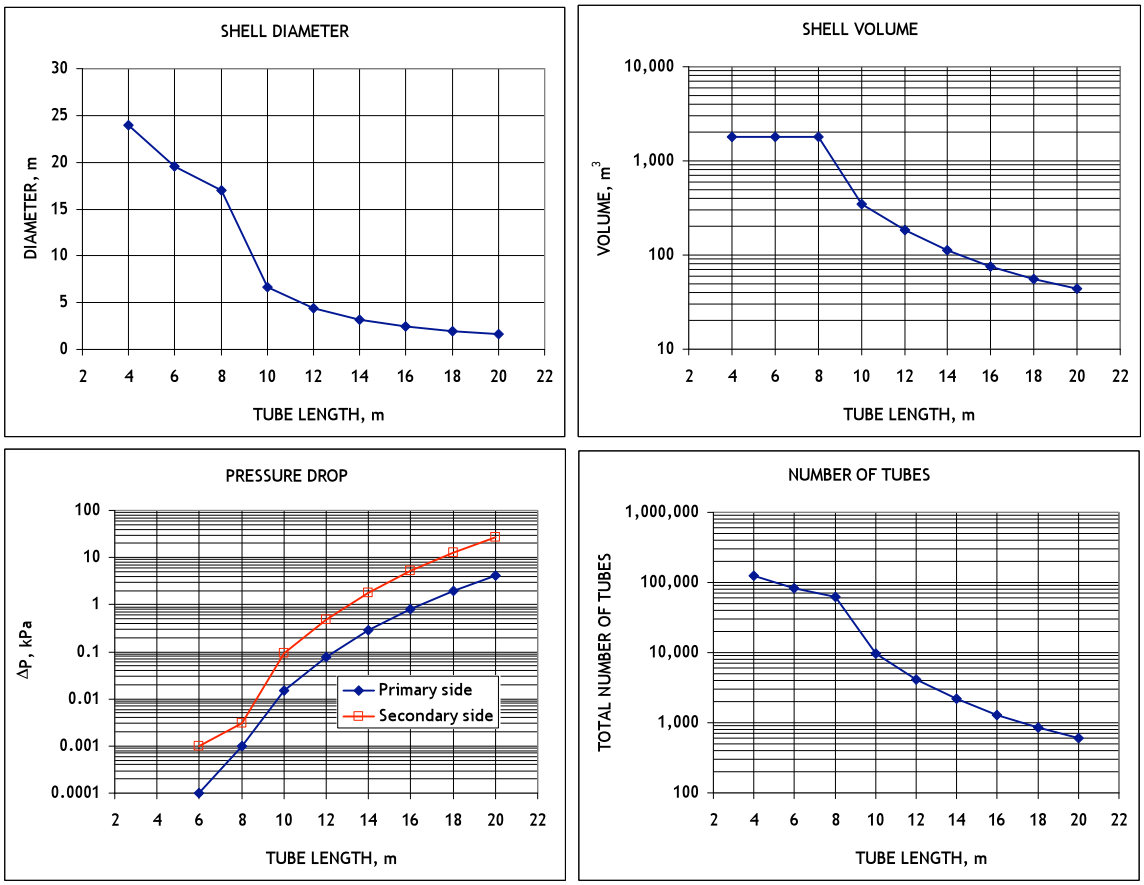

Figure 2.5. Shell-and-tube design sensitivity on the tube length for 3.5 cm tube.

2.1.5 Printed Circuit Heat Exchanger

The Printed Circuit Heat Exchanger (PCHE) calculations similar to those carried out in previous work [Natesan et al 2006] have been repeated for the thermal loading conditions of HCHX. Compared to the previous approach, some design modifications were made in the present study to satisfy the IHX requirements. In particular, the channel diameter was increased to 3.0 mm (compared to 1.6 mm used in the earlier study) and channel zigzag angle was decreased to 30° (compared to 90° and 45° used earlier) in order to satisfy the pressure drop design requirements (50 kPa on each side). Consequently, both plate thickness and channel pitch were increased since the pitch-to-diameters and plate thickness-to-channel diameter ratios are assumed to be the same for these calculations, as in the previous work.

The resulting PCHE parameters are presented in comparison with helical coil and shell-and-straight tube designs in Table 2.7 in the next section.

2.1.6 Comparison of the Heat Exchanger Designs

Table 2.7 compares the main design parameters and calculated conditions for helical coil, shell-and-tube, and printed circuit heat exchanger. The results presented in Table 2.7 are for one 178 MWt heat exchanger; three times more units will be required for the entire plant according to Table 2.3. Note that in HX volume comparison, the HCHX has an inner pipe such that the actual heat transfer volume is somewhat smaller than the total heat exchanger volume reported in Table 2.7.

Table 2.7. Comparison of the heat exchanger concepts

	Helical Coil	Shell-and-Tube		PCHE
		1 cm tube	3.5 cm tube	
Number of units	1	1	1	9
Tube inner (channel) diameter, mm	35.0	10.0	35.0	3.0
Tube (min. plate) thickness, mm	5.0	2.0	5.0	1.0
Tube (channel) pitch, mm	65.0	20.22	65.0	1.5
Tube (channel) length, m	22.1	4.0	12.0	0.39
Number of tubes	552	9,621	4,192	-
HX length*, m	4.60	4.0	12.0	0.6
HX cross section, m	4.08 D	2.08 D	4.42 D	0.6 H x 1.5 W
Unit volume*, m^3	60.14	13.62	183.96	0.54
Total HX volume*, m^3	60.14	13.62	183.96	4.86
Primary side pressure drop, kPa	2.024	1.577	0.077	44.351
Secondary side pressure drop, kPa	37.05	15.774	0.486	36.951

*For tubular design, only length of heat transfer region is given (i.e., headers are excluded)

3 Stress Calculations in Gas-to Gas IHX

3.1 Helical IHX

Although thermal and stress analyses of a three-dimensional spiral structure like the helical IHX are complex, since its basic component consists of a thin walled tube, rules of Subsection NH of the ASME Code can be applied. The outer diameter and wall thickness of the tube are 45 mm and 5 mm, respectively.

For the purpose of the present report, a single 4.6 m long (excluding the header regions at the inlet and outlet ends) average helical IHX is considered. A finite element model of the IHX for thermal conduction analysis is shown in Fig. 3.1. The helix diameter and pitch are 3.128 m and 65 mm, respectively. The base case with the reactor outlet temperature of 900°C, the reactor outlet pressure of 7 MPa, and the intermediate loop pressure of 7.1 MPa is considered for stress analysis. First, a steady-state thermal conduction analysis was carried out using the heat transfer data for both the hot and cold sides of the helical tube as a function of axial location. Next stress analyses were conducted with and without thermal stress contribution.

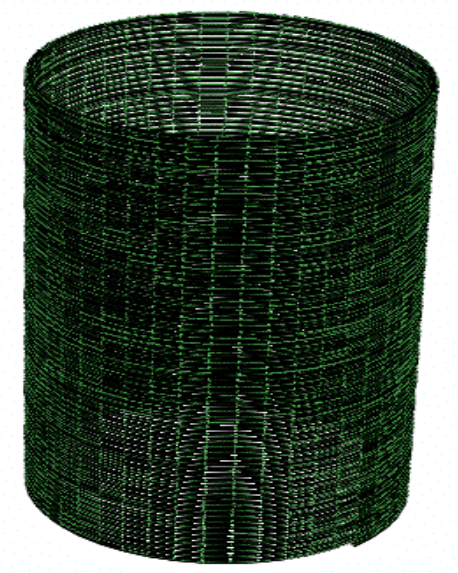

Figure 3.1. Finite element model of a helical IHX.

3.1.1 Thermal Conduction Analysis

The structural material considered was Alloy 617 whose thermal conductivity was input as a function of temperature in the finite element code (ABAQUS). The HTC and gas temperature data at inner diameter (ID) and outer diameter (OD) surfaces of the helical IHX were input in the FEM as functions of vertical (axial) location.

The FEA-calculated distribution of temperatures at the hot side (OD surface) and cold side of the tube are plotted in Figs. 3.2 and 3.3, respectively. Note that the temperature gradient at each end from the hottest to the coldest point is small (≈30°C). However, there is a large axial temperature gradient from the hot to the cold end, as expected. The maximum and minimum structure temperatures are 775 and 347°C, respectively. For comparison, the maximum and minimum structure temperatures calculated by the thermal hydraulics analysis are 779°C and 359°C, respectively. Detailed temperature distributions near the hot end and cold end of the IHX are plotted in Figs. 3.4 and 3.5, respectively.

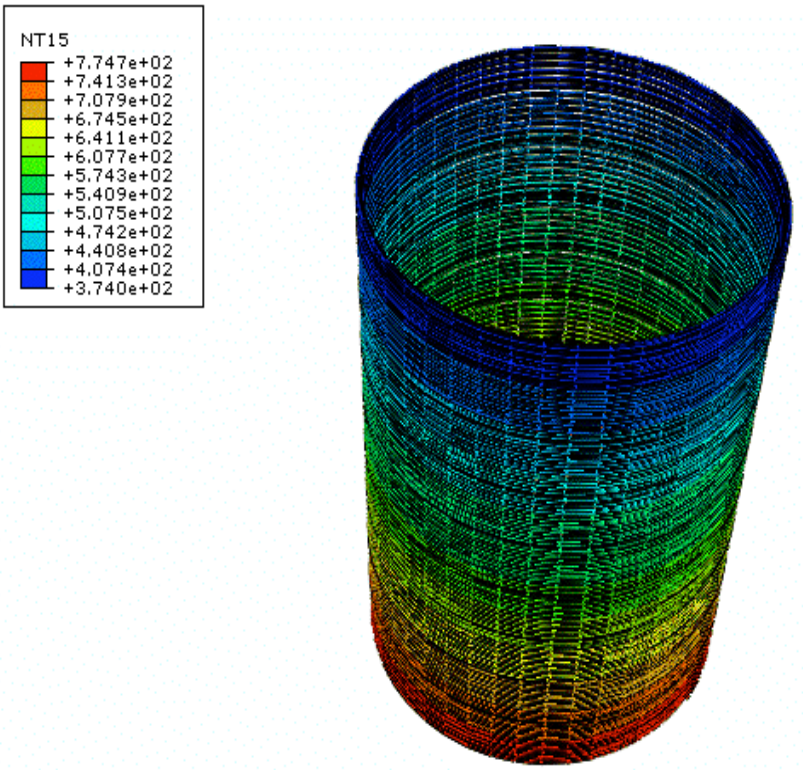

Figure 3.2. Temperature distribution in the helical IHX at the outer surface (hot side).

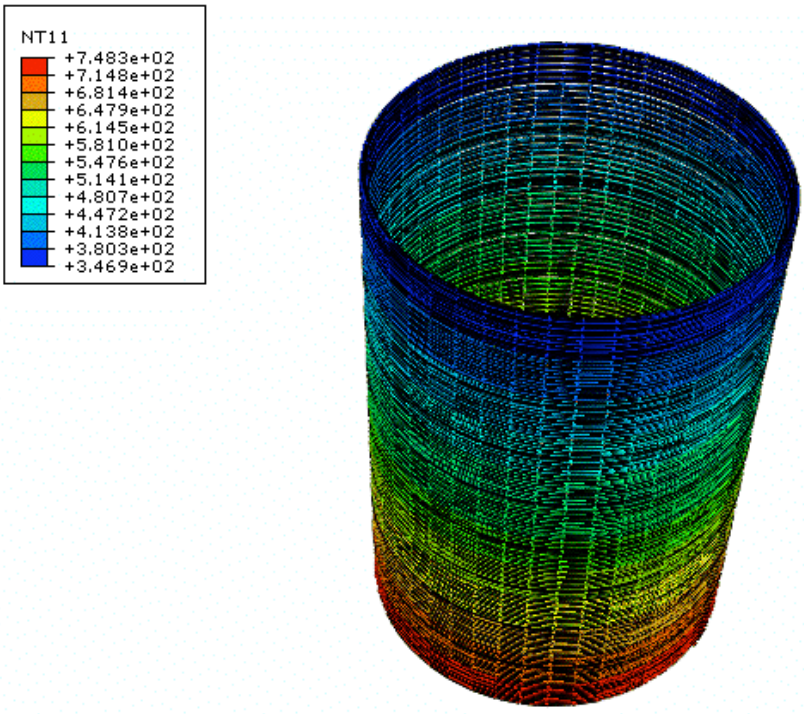

Figure 3.3. Temperature distribution in the helical IHX at the inner surface (cold side).

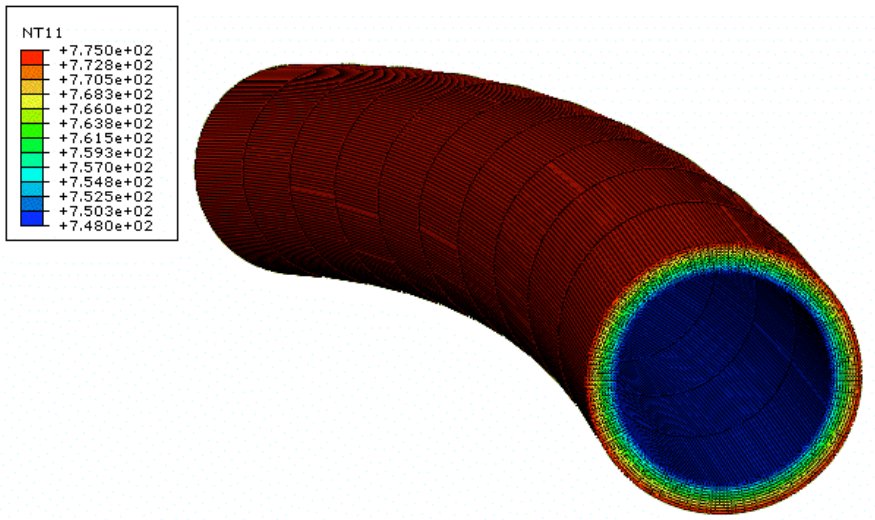

Figure 3.4. Detailed temperature distribution in the helical IHX at the hot end.

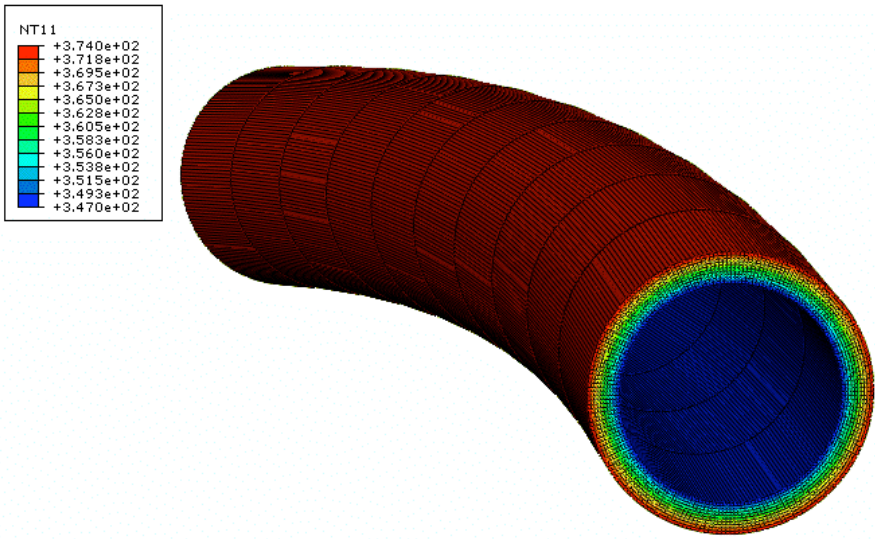

Figure 3.5. Detailed temperature distribution in the spiral IHX at the cold end.

3.1.2 Stress Analyses

Two stress analyses, both assuming linear elastic behavior, were conducted using the finite element code ABAQUS. First, a primary (pressure) stress analysis was conducted without any contribution from thermal stresses. Second, a secondary (thermal) stress analysis was conducted without the pressure stresses. In the second analysis, the temperature data calculated in the thermal conduction analysis (Section 3.1.1) were input into the ABAQUS code. For the stress analysis, the IHX at each end was analyzed as a donut-shaped ring.

3.1.2.1 Primary Stress Analysis

The primary stress distribution in the IHX is shown in Fig. 3.6. As expected, the stresses are very low due to the small pressure drop from the ID to the OD side of the tube. The maximum von Mises effective stress is 0.4 MPa, which is approximately uniform over the entire IHX.

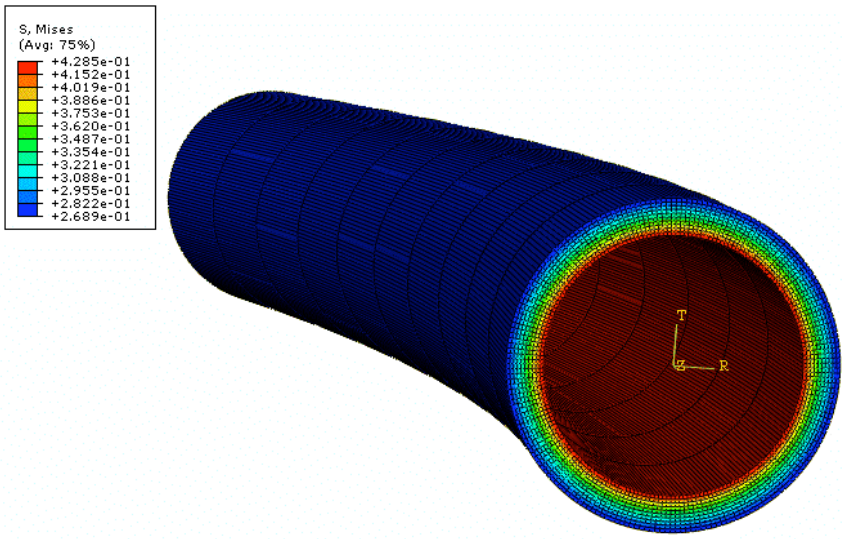

Figure 3.6. Distribution of primary (pressure) von Mises effective stress at either end of the helical IHX.

3.1.2.2 Secondary Stress Analysis

The distribution of effective von Mises stress at the hot and cold ends of the IHX due to thermal loading are plotted in Figs. 3.7 and 3.8, respectively. A peak stress of 58 MPa occurs at the hot end and a peak stress of 54 MPa occurs at the cold end.

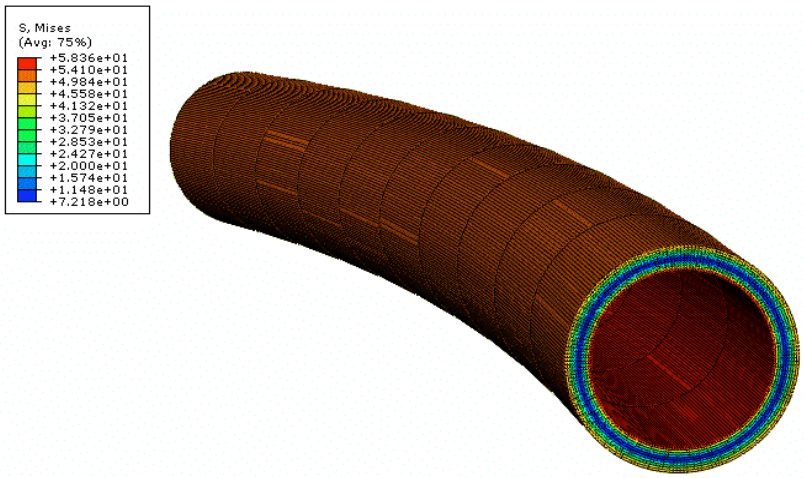

Figure 3.7. Distribution of von Mises effective stress due thermal loading at the hot end of the helical IHX.

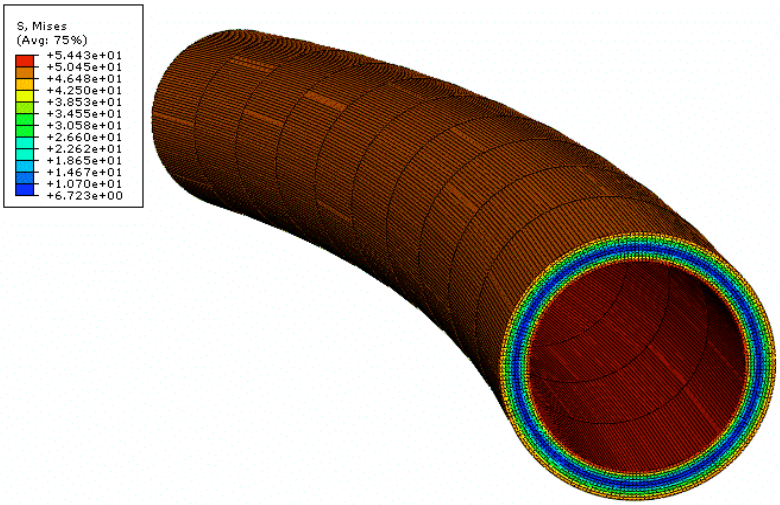

Figure 3.8. Distribution of von Mises effective stress due to thermal loading at the cold end of the helical IHX.

3.1.3 ASME Code Compliance Calculations

Since the IHX operates in a high temperature environment where creep deformation is important, Subsection NH of ASME Code, Section III is applicable. However, the use of the primary candidate structural Alloy 617 is currently not approved in Subsection NH. There is a draft Code Case (still unapproved) for designs using Alloy 617. The draft Code Case was patterned after relevant portions of Subsection NH, and limited to Alloy 617, temperature of 982°C (1800°F), and maximum service life [total life at temperatures above 427°C (800°F)] of 100,000 h or less. However, the ratcheting rules in the draft Code Case is limited to a maximum temperature of 649°C. The draft Code Case focused on Alloy 617 because it was a leading candidate high-temperature structural material, and there was a significant material properties database at the temperature of interest. We have used the allowable stress values from this draft Code Case for the present report.

3.1.3.1 Primary Stress Limits

A basic high temperature primary stress limit is S_{mt}, which is the lesser of S_m and S_t, and is a function of both time and temperature. For nickel-based alloys, S_m is basically defined as follows:

$$S_m = \min \begin{cases} \frac{1}{3} S_u \\ \frac{2}{3} S_y \end{cases} \tag{3.1}$$

where S_u is the lesser of ultimate tensile strength at temperature and the minimum ultimate tensile strength at room temperature, S_y is the lesser of yield strength at temperature and the minimum yield strength at room temperature. For each specific time t and temperature T, S_t is defined as the least of the following three stresses:

(1) 100% of average stress to obtain a total (elastic, plastic, and creep) strain of 1%,
(2) 80% of the minimum stress to cause initiation of tertiary creep, and (3.2)
(3) 67% of the minimum stress to cause rupture.

In the draft code case for Alloy 617, the condition (2) above is dropped because nickel-base alloys do not exhibit classical (i.e., primary, secondary, and tertiary) creep behavior. The reported S_m and S_t values for Alloy 617 are plotted in Fig. 3.9. To apply the code rules for primary stresses, primary membrane and bending stresses have to be determined first. However, in the case of the helical IHX the primary stresses are so low (<1 MPa) that they easily satisfy the primary stress limits corresponding to 10^5 hours at 775°C (Fig. 3.9).

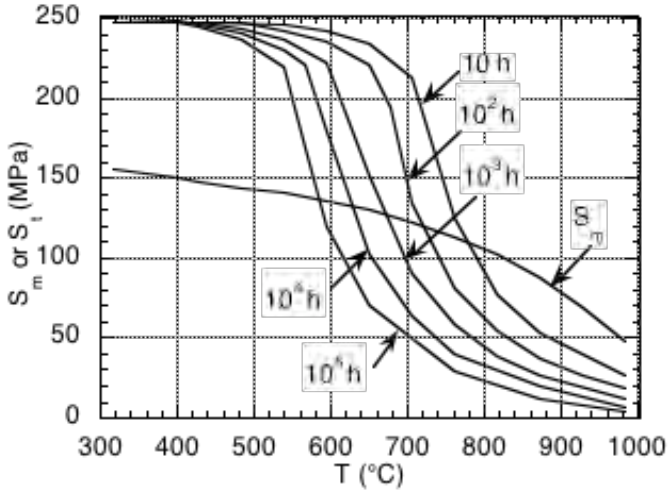

Figure 3.9. Variation of S_m and S_t of Alloy 617 with temperature and time.

3.1.3.2 Primary Plus Secondary Stress Limit

The primary plus secondary stress limits were checked at the hot end and the cold end. A summary of the stresses at these locations is given in Table 3.1.

Table 3.1. Summary of primary and secondary stresses in HCHX at the cold and hot ends

Location	$P_L + P_b$ (MPa)	Q (Mpa)	T (°C)	S_y (Mpa)	X	Y
Cold end	0.4	54	360	238	0.001	0.23
Hot end	0.4	58	770	279	0.001	0.21

Ratcheting Limit

One of the available tests in Subsection NH for satisfying the ratcheting strain limit is Test no A2.

Test No. A2

$$X + Y \leq 1 \qquad (3.3)$$

for those cycles during which the average wall temperature at one of the stress extremes defining the maximum cyclic primary plus secondary stress range is below the temperature where creep is negligible. In Eq. 1.3,

$X=(P_L + P_b)/S_y$ or P_m/S_y and $Y=Q/S_y$ where Q=secondary stress intensity range.

Assuming that the low temperature end of the temperature cycle is below the creep range, it can be verified that Test No. A2 is satisfied for both locations considered in Table 1.1. However, according to the draft code case for Alloy 617, the behavior of Alloy 617 above 650°C is such that simple ratcheting rules like Test No A2 may not be applicable. New rules are needed in this temperature range.

Creep-Fatigue Limit

Creep-fatigue life of the IHX will be influenced by the peak stresses created by the interaction of the header region with the helical core which was not included in the FEM. The creep and fatigue curves given in the draft code case do not include the effects of impure helium environment. Currently the design fatigue cycles for the IHX are not well established and therefore, fatigue and creep-fatigue life analyses were not performed.

3.2 Shell and Straight Tube Heat Exchanger

We have analyzed the base case for the reference deign of the shell and tube IHX which consists of 12-m long, 35-mm ID, and 45-mm OD Inco Alloy 617 tubes arranged in a triangular lattice inside a shell. The reactor outlet temperature and pressure are 900°C, and 7 MPa, respectively and the secondary side pressure is 7.1 MPa and the inlet cold temperature is 308°C.

The shell and tube design is relatively easy to analyze. A single tube without the header region is considered for analysis (Fig. 3.10). The interaction of the header region with tube, which will add some complications to the analyses, is ignored for the present. In all cases, the axial displacement (u_Z) was set equal to zero at one end (z=0) and generalized plane strain deformation (i.e., u_Z=constant) was assumed at the other end.

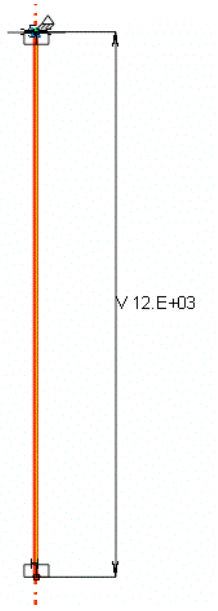

Figure 3.10. Tube analyzed for the shell and tube design.

3.2.1 Thermal Conduction Analysis

Thermal conduction analysis was conducted with the HTCs and gas temperatures at the OD and ID surfaces prescribed as functions of axial location. Detailed temperature distributions

at the hot and cold ends are plotted in Figs. 3.11 and 3.12, respectively. The temperature gradient at each end is small (8°C). As for the helical design, there is a large temperature gradient from the hot to the cold end. The maximum temperature is 775°C, which is the same as that for the helical design. However, the minimum temperature of 365°C is higher than that for the helical design (347°C).

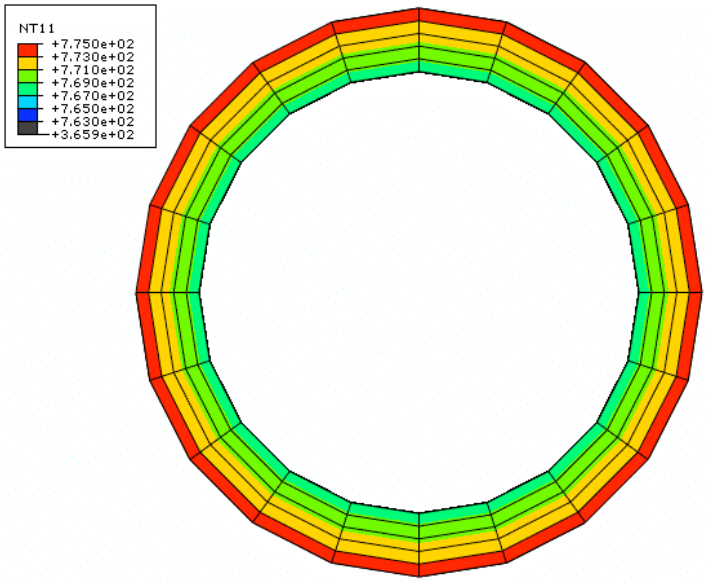

Figure 3.11. Detailed temperature distribution in the tubular IHX at the hot end.

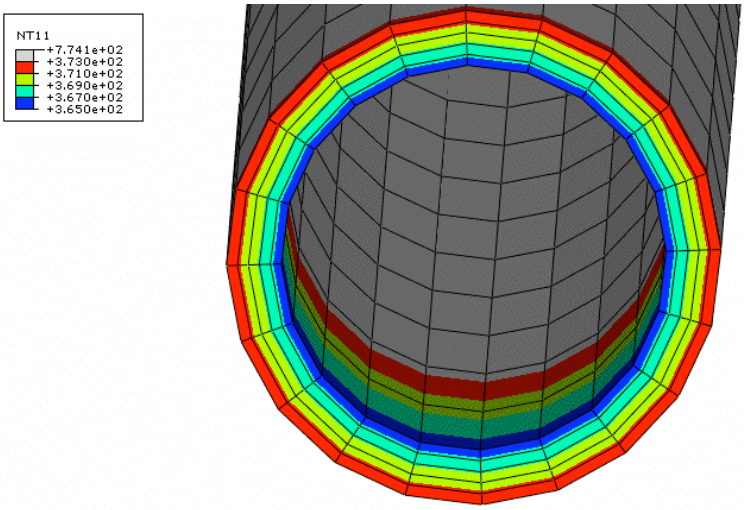

Figure 3.12. Detailed temperature distribution in the tubular IHX at the cold end.

3.2.2 Primary Stresses

The membrane primary stress intensity (P_m) due to the base case primary and secondary side pressures is 6.9 MPa (Fig. 3.13) and the maximum average wall temperature at the hot end is 770°C. The calculated values of P_m and $P_L + P_b$ are plotted on the allowable stress intensities vs. time and temperature plot for Alloy 617 in Fig. 3.14. It is evident that the design life is significantly greater than 10^5 h.

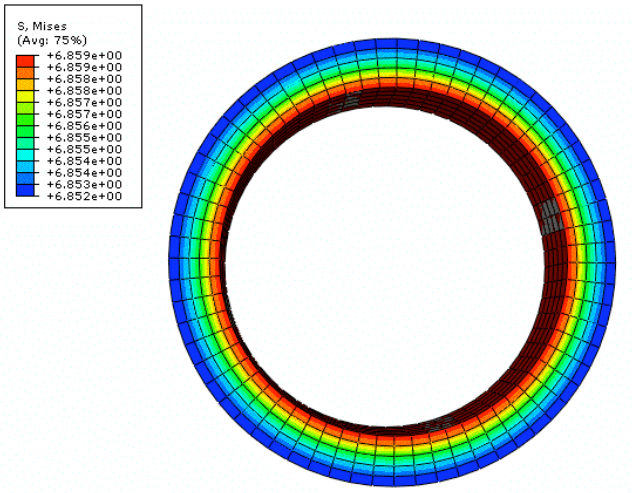

Figure 3.13. Distribution of primary (pressure) von Mises effective stress at either end of the helical IHX.

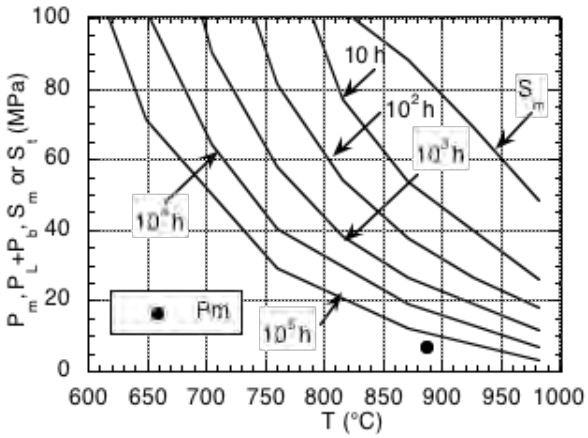

Figure 3.14. Calculated P_m and $P_L + P_b$ values for the shell and tube IHX plotted on the allowable stress intensities vs. temperature and time curves for Alloy 617.

3.2.3 Primary Plus Secondary Stresses

The distribution of thermal stress intensity (Q) at the hot and cold ends are plotted in Figs. 3.15 and 3.16, respectively. Variation of the primary membrane (P_m) and maximum secondary stress intensities (Q) in the tube axial direction is shown in Fig. 3.17.

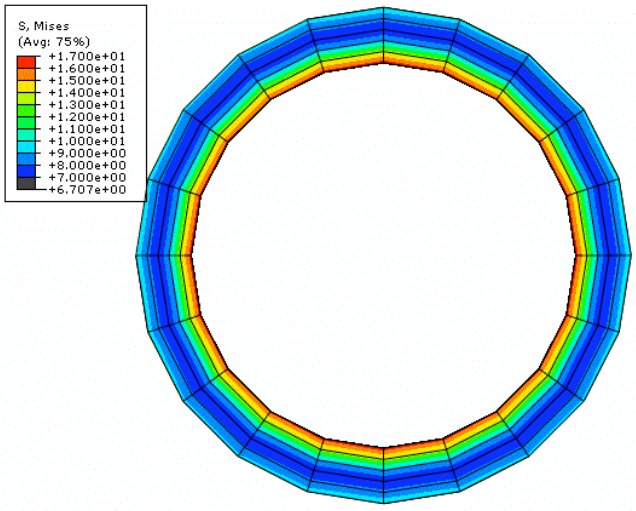

Figure 3.15. Distribution of von Mises effective stress due thermal loading at the hot end of the tubular IHX.

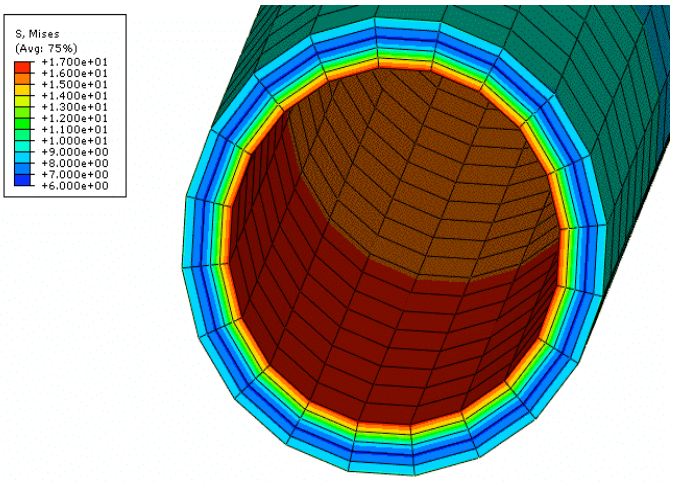

Figure 3.16. Distribution of von Mises effective stress due to thermal loading at the cold end of the tubular IHX.

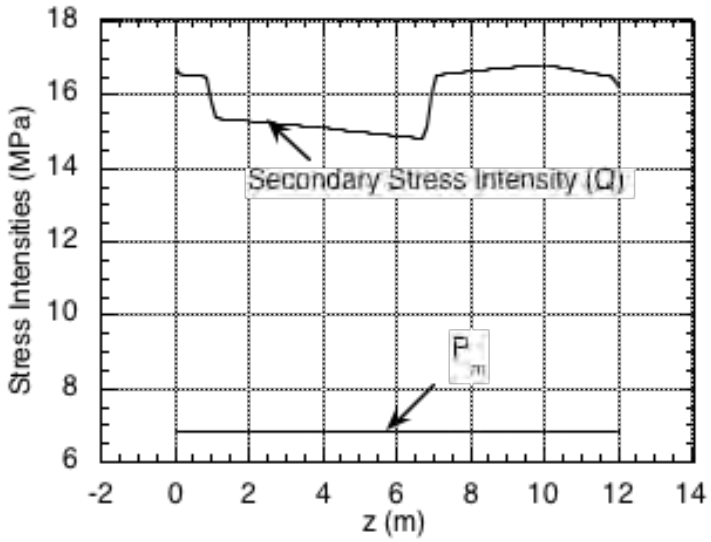

Figure 3.17. Variation of P_m and Q along the length of the tube.

Ratcheting Limit

As in Section 5.1.3.2 of the earlier report [Natesan et al 2006], assuming that the low temperature end of the temperature cycle is below the creep range, Test No. A2 (Eq. 3.3) is applied. A plot of the variation of the value of X+Y and average temperature with axial location is plotted in Fig. 3.18 that shows that Test A2 (Eq. 3.3) is satisfied at all axial locations.

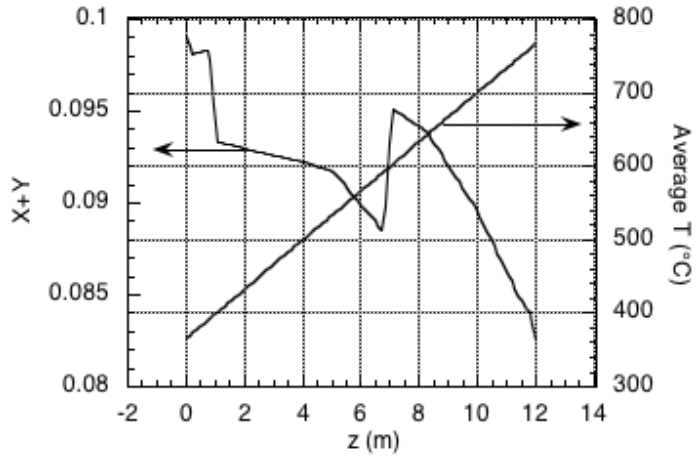

Figure 3.18. Variation of X + Y and average T along the length of the tube.

4. Summary

Preliminary thermal and stress analyses have been conducted for the helical gas-to-gas IHX and the 12 m long shell and straight tube gas-to-gas IHX, ignoring any interaction with the header regions. The header regions have to be included in the analyses, because interaction between the core structure and the header regions may lead to high local stresses.

Analyses of simplified geometries of the core region of both designs conducted in this report show that both designs, using Alloy 617 as the structural material, satisfy the primary stress and ratcheting stress limits for the base case. However, it should be noted that the ratcheting rules in the Draft Code Case for Alloy 617 are limited to temperatures <650°C, which is violated in the base case. Therefore, new ratcheting rules are needed for the IHX.

For a reactor outlet temperature and pressure of 900°C and 7 MPa, respectively, and a secondary side inlet temperature and pressure of 308°C and 7.1 MPa, respectively, the allowable design life (based on in-air tensile and creep rupture strengths of Alloy 617) is $>10^5$ h for both the helical and the 12 m long shell and tube IHX. Because of the low primary stress, the 4 m long shell and tube design should also behave in a similar fashion. These calculations are based on analyses of the IHX core; further reduction in life may result from interaction of the core region with the header regions, which is not included in the present analyses.

It should be noted that the above lifetimes are based on creep rupture data of Alloy 617 in thick sections in air. If tests show that exposure to high temperature impure helium leads to significant reduction of creep rupture life compared to that in air, the design lifetimes will be reduced. The design lives may also have to be reduced to account for thickness effect.

5. References

AREVA 2008, “NGNP with Hydrogen Production. IHX and Secondary Heat Transport Loop Alternatives,” AREVA NP Inc., Document No. 12-9076325-001, April 2008.

Davis, C. B., Oh, C. H., Barner, R. B., Sherman, S. R., and Wilson, D. F., 2005, “Thermal-Hydraulic Analyses of Heat Transfer Fluid Requirements and Characteristics for Coupling A Hydrogen Production Plant to a High-Temperature Nuclear Reactor,” INL/EXT-05-00453.

General Atomics 2008, “Engineering Services for the Next Generation Nuclear Plant (NGNP) with Hydrogen Production. NGNP IHX and Secondary Heat Transport Loop Alternatives Study,” Prepared by General Atomics For the Battelle Energy Alliance, LLC, 911119, Revision 0, April 2008.

Generation IV International Forum, 2002, A Technology Roadmap for Generation IV Nuclear Energy Systems, FIF-002-00.

Harvego, E. A., 2006, “Evaluation of Next Generation Nuclear Power Plant (NGNP) Intermediate Heat Exchanger (IHX) Operating Conditions,” Idaho National Laboratory Report INL/EXT-06-11109.

Independent Technology Review Group, 2004, Design Features and Technology Uncertainties for the Next Generation Nuclear Plant, Idaho National Laboratory Report INEEL/EXT-04-01816.

Lillo, T. M., Williamson, R. L., Reed, T. R., Davis, C. B., and Ginosar, D. M., 2005, Engineering Analysis of Intermediate Loop and Process Heat Exchanger Requirements to Include Configuration Analysis and Materials Needs, Idaho National Laboratory Report INL/EXT-05-00690.

McDonald, C. F., 1996, “Compact Buffer Zone Plate-Fin IHX- Key Component for High-Temperature Nuclear Process Heat Realization With Advanced MHR,“ Applied Thermal Engineering, 16, p.32.

Natesan, K., A. Moisseytsev, S. Majumdar, and P. S. Shankar, “Preliminary Issues Associated with the Next Generation Nuclear Plant Intermediate Heat Exchanger Design,” ANL/EXT-06/46, Argonne National Laboratory, 2006.

Smith, E. M., “Thermal Design of Heat Exchangers, A Numerical Approach: Direct Sizing and Stepwise Rating”, John Wiley & Sons, Chichester, 1997.

Nuclear Engineering Division
Argonne National Laboratory
9700 South Cass Avenue, Bldg. 212
Argonne, IL 60439-4838

www.anl.gov

UChicago ▶ Argonne LLC

A U.S. Department of Energy laboratory
managed by UChicago Argonne, LLC